Macromolecular
Materials and Engineering
www.mme-journal.de

Overview of the Experimental Trends in Water-Assisted Injection Molding

Xianhu Liu, Yamin Pan, Guoqiang Zheng, Hu Liu, Qiang Chen, Mengyao Dong, Chuntai Liu,* Jiaoxia Zhang, Ning Wang, Evan K. Wujcik, Tingxi Li, Changyu Shen,* and Zhanhu Guo**

A Dedication to NERC-APPT for 30 years

In recent years, a new and promising polymer processing technology known as water-assisted injection molding (WAIM) has attracted attention not only for academic reasons but also for its industrial applications. WAIM technology provides a new way to fabricate hollow or other complicated products due to its faster cycling time and light weight. This paper aims to give an overview of the basic principles and applications of WAIM as well as the current research status in academia. The origin and development of WAIM technology are first described and then, their advantages and applications are given. This review focuses on the experimental trends of WAIM such as computer simulation, the effect of processing parameters on the WAIM samples, and the morphology as well as related WAIM–molded composites and polymer blends' work.

1. Background

In the early 1970s, the idea of injecting the fluid into polymer melts in the mold was proposed to produce hollow parts, and later the Water-Assisted Injection Molding (WAIM) technology was developed.[1–14] WAIM technology, one of the latest and most promising technologies, has received extensive attention in recent years, due to the lightweight of its products, relatively lower resin cost per part, faster cycle time, and its flexibility in the design and manufacture of hollow plastic parts.[1–5] However, due to the development and wide applications of gas-assisted injection molding (GAIM),[6–9] WAIM had been set aside in the last century. It bursts onto the scene in a big way at fall's K 2001 show, which was stimulated by a report on WAIM research by the researchers at Institute of Plastics Processing (IKV), Germany.[10–14] Since then, WAIM has been widely investigated in industry and academia.

Up to now, great efforts have been made toward the simulation and investigation of WAIM process as well as the development of WAIM equipment. IKV is one of the pioneering groups on WAIM. Michaeli et al. systematically investigated the injector technology, residual wall thickness, and hollow space formation during the WAIM process.[10–18] In addition, some researchers simulated the WAIM process using interesting approaches.[19–22] Liu first reviewed the development and progress of WAIM technology in 2009.[1] This review focused on the WAIM equipment and the water penetration behavior and simulation, but it did not provide

Dr. X. Liu, Dr. H. Liu, M. Dong, Prof. C. Liu, Prof. C. Shen
National Engineering Research Center
for Advanced Polymer Processing Technology (NERC-APPT)
Zhengzhou University
Zhengzhou 450002, China
E-mail: ctliu@zzu.edu.cn; shency@zzu.edu.cn

Dr. Y. Pan, Prof. G. Zheng, Prof. C. Shen
College of Material Science and Engineering
Zhengzhou University
Zhengzhou 450001, China
E-mail: yamin.pan@fau.de

Dr. H. Liu, M. Dong, Dr. J. Zhang, Prof. Z. Guo
Integrated Composites Laboratory (ICL)
Department of Chemical & Biomolecular Engineering
University of Tennessee
Knoxville, TN 37996, USA
E-mail: zguo10@utk.edu

The ORCID identification number(s) for the author(s) of this article can be found under https://doi.org/10.1002/mame.201800035.

DOI: 10.1002/mame.201800035

Dr. Q. Chen
State Key Laboratory of Solidification Processing
Northwestern Polytechnical University
Xi'an, Shaanxi 710072, China

Dr. J. Zhang
School of Material Science and Engineering
Jiangsu University of Science and Technology
No 2, Mengxi Rd, Zhenjiang, Jiangsu 212003, China

Prof. N. Wang
State Key Laboratory of Marine Resource Utilization in South China Sea
Hainan University
Haikou 570228, China

Prof. E. K. Wujcik
Materials Engineering and Nanosensor [MEAN] Laboratory
Department of Chemical and Biological Engineering
The University of Alabama
Tuscaloosa, AL 35487, USA

Prof. T. Li
College of Materials Science and Engineering
Shandong University of Science and Technology
Qingdao 266590, China

the experimental trends on WAIM. Furthermore, there have been investigations on the morphology and orientation evolution of the WAIM parts recently.[23–27] Therefore, the present review article aims to review and summarize current research in WAIM, focusing on experimental trends in computer simulation, the effect of processing parameters, morphology and orientation, fiber-filled thermoplastic composites, as well as the polymer blends. Before that, we first introduce the schematic, WAIM equipment, advantages and disadvantages, as well as the industrial applications of WAIM technology.

2. WAIM Technology

2.1. Schematic of WAIM Technology

Generally, according to the volume of injected melt, WAIM can be divided into short-shot process and full-shot process. A schematic diagram of short-shot process is illustrated in **Figure 1**. Clearly, it can be divided into three stages. First, the cavity is partially filled with polymer melt; second, the high-pressure water is injected into the core of the polymer melt; third, water continues to pack the melt till the melt is solidified. There are also some other WAIM processes, such as melt-push-back and core-pull back processes. The details of the WAIM process are provided in the refs. [1,28].

2.2. WAIM Equipment

WAIM equipment mainly comprises of a water-assisted injection unit, water injection pin, injection molding machine, and mold. Water-assisted injection unit supplies the pressurized water for the WAIM process. It generally includes a water pump, a water tank equipped with a temperature regulator, and a control circuit.[29] It has its own hydraulic and control system, and can be adapted to all molding machines (**Figure 2**). Water can be directly injected into the cavity via water injection pin.

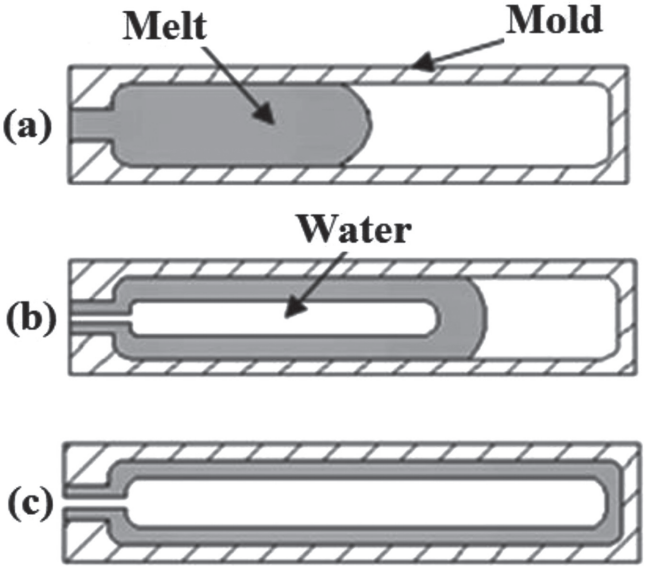

Figure 1. Schematic of short-shot WAIM process.

Xianhu Liu received his Ph.D. degrees respectively from Zhengzhou University in Henan, China, and Friedrich-Alexander-University Erlangen-Nuremberg in Erlangen, Germany. He is currently an associate professor at the National Engineering Research Center for Advanced Polymer Processing Technology in Zhengzhou University, China. His most recent interests concern the development of new polymer processing technology, polymer rheology and processing, preparation of advanced polymer composites as well as oil/water separation materials.

Chuntai Liu received his B.S. and M.S. respectively from Beijing University and Xi'an Jiaotong University, and his Ph.D. from Zhengzhou University. He joined the Zhengzhou University as a research scientist in 1990 and became a full Professor in 2003. He was visiting scholar at Ohio State University during 2006–2007. His research focuses on computer aided engineering for polymer processing and lightweight of automobiles.

Zhanhu Guo, an Associate Professor in the Department of Chemical and Biomolecular Engineering, University of Tennessee, Knoxville, USA, obtained a Ph.D. degree in Chemical Engineering from Louisiana State University (2005) and received three-year (2005–2008) postdoctoral training from the Mechanical and Aerospace Engineering Department at the University of California Los Angeles. Dr. Guo chaired the Composite Division of the American Institute of Chemical Engineers (AIChE, 2010–2011) and directs the Integrated Composites Laboratory. His current research focuses on multifunctional nanocomposites.

There are two types of water pin designs: movable type pin and stationary type pin. The former usually requires a more complex mold design and therefore is a challenge for the molders and the cost of mold is very high; the latter is a relatively easy and low cost mode, but it needs a targeted design for product. Water injection pin is the key factor to determine the success or

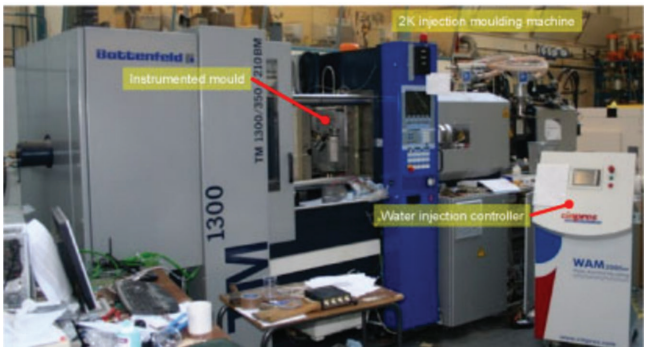

Figure 2. The commercially available water-assisted injection systems. Reproduced with permission.[19] Copyright 2008, Taylor & Francis.

failure of a part during the WAIM process, and up to now it is still a big problem in WAIM technology. In addition, although a large number of WAIM systems are commercially available (Figure 2), the cost of equipment is still very high.

2.3. Advantages and Disadvantages

WAIM is an important manufacturing technology with its potential still to be realized. The use of water as the internal fluid offers a number of significant advantages and new possibilities as compared with the currently well-established GAIM. The thermal conductivity of water is 40 times greater than that of gas, and the heat capacity of water is four times greater than gas.[3,4] With the cooling capability of water, the cooling cycle time of WAIM can be reduced to 50% than that of GAIM. Meanwhile, compared to gas, water has a higher viscosity and is incompressible, therefore, it can produce better-shaped hollow parts with good control and smoother surfaces (**Figure 3**). In WAIM, water compresses plastics into uniform and thinner residual walls ≈25% thinner than that in the typical GAIM. The uniformity of residual wall thickness around bends and other geometric shapes is a particular advantage of WAIM. Thinner residual walls directly correlate to materials savings; uniform residual wall thickness can directly lead to a uniform strength. In addition, the cooling from both inside and outside provides a more balanced cooling, resulting in a reduced postejection warpage.

Due to the involved additional processing parameters, the molding window and process control are more critical and difficult. Therefore, WAIM has some limitations. For example, the removal of water after molding is a major obstacle for the popularization and application of WAIM technology. During the molding process, the presence of water may corrode the steel mold. **Table 1** lists the advantages and disadvantages of the WAIM.

2.4. Industrial Applications

WAIM has been under development for more than 20 years and is already successfully commercialized. Majority of them are in Europe, where WAIM originated. Badische

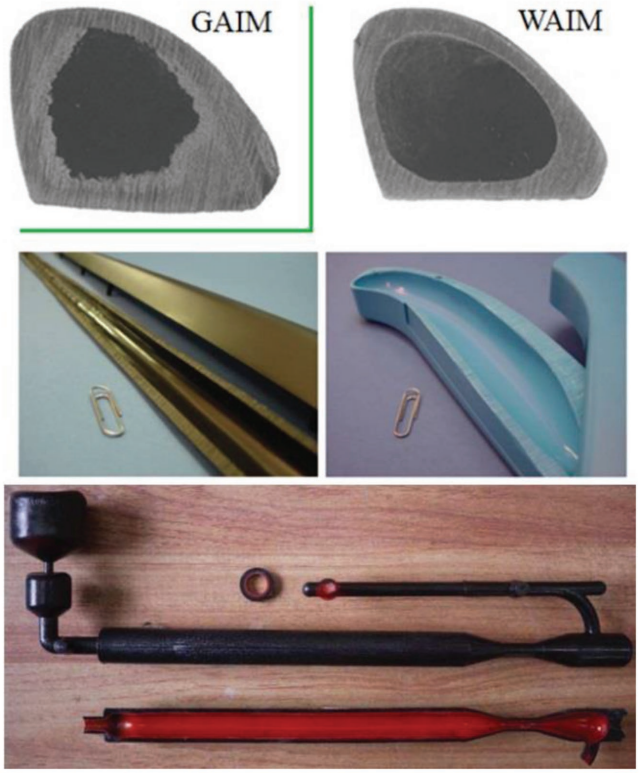

Figure 3. Smooth surfaces of internal channels of GAIM and WAIM parts.[30] Copyright 2016, Wiley-VCH.

Ailin-und-Soda-Fabrik (BASF) has already optimized several resin grades specifically for use in WAIM, and for several product applications. The first commercial use of Battenfeld's Aquamold system started 2005 with the handlebar and front-wheel fork of a new tricycle from Smoby SA of France.[4]

WAIM is especially well suited for a number of hollow-part applications, such as automotive fluid handling tubes for

Table 1. Advantages and disadvantages of WAIM technology.

Advantages	Disadvantages
1. Shorter cycle time	1. Not suitable for multicavity
2. Smooth inner surface	2. Corrosion of the steel mold due to water
3. Uniform residual wall thickness	3. Removal of water after molding
4. Minimal warpage and shrinkage	4. Increased mold sealing requirement
5. Flexibility in the design and manufacture of plastic parts	5. Some materials are difficult to be molded
6. Eco-friendly due to the used water	6. Not suitable for high temperature injection molding
7. Reduced material consumption due to the hollow structure of hte parts	7. Larger orifices of injection pin required (easier to get stuck by the polymer melt)
8. Low cost of water (water is much cheaper and can be easily recycled)	8. Difficult to predict residual wall thickness depending on part geometry and polymer used
9. No internal foaming phenomenon	

oils and coolants, automotive door handles, oven and refrigerator handles, chain saw handles, and office furniture chair arms. Teklas, a Turkish supplier to the automotive industry, has actively pushed the development of WAIM technology for manufacturing hollow plastic parts. For example, glass fiber (GF)–reinforced polyamide 66 (PA66) tube with good inside and outside surfaces as well as the required high chemical resistance has been successfully developed by WAIM. In addition, by using the WAIM technology, Teklas is able to manufacture a variety of tube shapes and combinations with different wall thicknesses and great complexity.

3. Current Research

3.1. Computer Simulation

Simulation is a useful tool for the mathematical modeling in polymer crystallization and processing.[31–34] Due to the complexity of the WAIM process,[35–37] computer simulation is expected to become an important and required tool to help understanding this process, especially tracing two moving interfaces which are the water–melt interface and melt–front interface. However, there are few reports on modeling and simulation of WAIM. Theoretically, the WAIM process is a 3D, transient, two-phase problem with moving front– and water–melt interfaces, this is somewhat similar to the GAIM process.[38–42]

The melts flow behavior, penetrated length, residual wall thickness, temperature, shear fields, and so on have been predicted based on the improved models.[43–54] Based on Hele–Shaw flow model (which is widely used in modeling conventional injection molding (CIM)), Li et al.[44] and Zhang et al.[45] studied the residual wall thickness of tubes through computer simulations, and Zhang et al.[46] put forward the model and numerical simulation method for the second penetration (water injection). They found the dependence of the residual wall thickness on the water pressure and melt temperature, which was consistent with the experimental data. Polynkin et al.[19] and Silva et al.[21] used the volume of fluid method to simulate the high-pressure water penetration and successfully traced the polymer–water interface. Recently, Wang et al.[22] used this method to simulate the process of high-pressure water penetration, and showed that the process of melt filling propelled by high-pressure water was divided into three stages: initial filling, fast filling, and terminal filling, and the water had a little shear effect on the melt in the water-penetrated zone. Yang et al.[47–49] found that the water penetration was uniform and smooth in the long straight water channel, and the wall thickness difference was small (**Figure 4**). However, it was easy to produce water fingering in variable cross-section and L-shaped water channels.[50]

A simulation model for the filling stage of a pipe cavity during the short-shot WAIM was proposed by Kuang.[51] It was found that the short-shot size was the principal parameters affecting the water penetration length, while melt temperature, mold temperature, water temperature, and water pressure were found to have little effect on the water penetration. In addition, Liu and Chen[52] used a transient heat transfer finite element model to simulate and predict the temperature variation of the WAIM products during the cooling process, and found that the simulated results matched well with the experimental data.

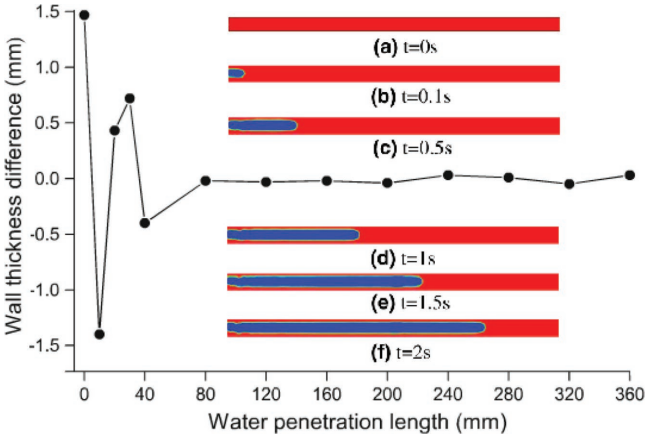

Figure 4. Residual wall thickness difference of long straight water channel and water/melt penetration interface. Reproduced with permission.[48] Copyright 2012, Springer.

In order to achieve a better pressure control performance of the injecting water to meet the requirements of the WAIM, the proportional pressure control of the WAIM system was reported both numerically and experimentally.[53,54] The simulation results indicate that a high flow area water injector is more suitable for the pressure control, and the increase of integrator gain could lead to overshoot and oscillation phenomena.

Additionally, Liu and Chen[55] and Liu and Su[56] used a proposed transient heat transfer finite element model to simulate and predict the temperature variation during WAIM process. The result showed that the temperature profiles of WAIM parts can be well predicted. Zheng et al.[27] used the hybrid finite element and finite difference method to simulate the evolution of temperature and shear stress during WAIM and CIM. The results demonstrate that the temperature and shear stress in the skin region decrease faster than these of water channel region (**Figure 5**). The simulation results account for the experimental results satisfactorily.

3.2. Effect of Processing Parameters

Despite the advantages associated with WAIM process, the molding window and process control become more critical and difficult since additional processing parameters are involved, such as water pressure, water delay time, and water injection time. Water penetration length and residual wall thickness significantly affect the quality of WAIM parts, therefore many researchers have investigated the effects of processing parameters as well as water pin form and channel geometry on the penetration length and residual wall thickness distribution by experiments and achieved lots of research findings.[57–62,68]

Part geometry, especially for the part with curved section and sudden dimensional transition, has an important effect on the water penetration length and residual wall thickness. The influences of the cavity cross-section shape (i.e., part geometry) and the processing parameters on the water penetration behavior

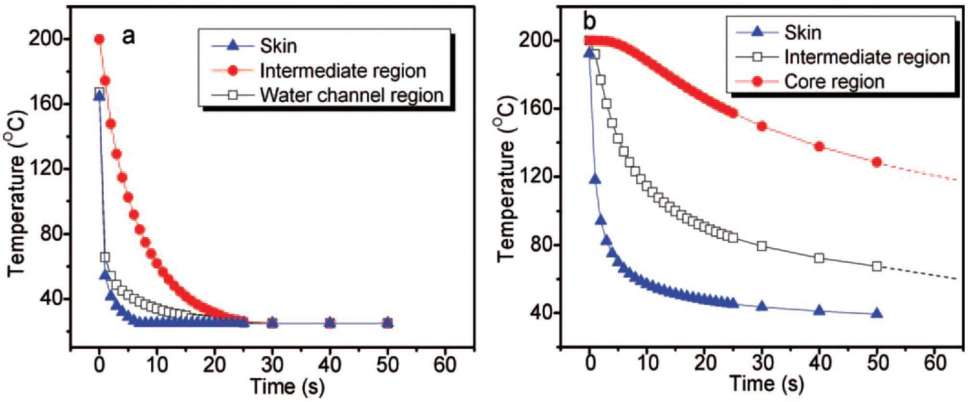

Figure 5. Simulated temperature profiles during a) WAIM and b) CIM for neat iPP.[27] Copyright 2012, Wiley-VCH.

were explored by Kuang et al.[30] For the circular pipe, the residual wall thickness was rather even, but for the noncircular pipes, the maximum residual wall thickness always occurred at the wall (the farthest from the center of the cross-section), as shown in **Figure 6**. Huang and Deng[63] investigated the influences of short-shot size, melt temperature, water injection delay time, and water pressure on the water penetration length and residual wall thickness of WAIM curved polypropylene (PP) pipe. They found that the short-shot size is the most effective factor, which is in good agreement with the simulation result.[51] Yang and Chu[64] and Liu and Hsieh,[65] respectively, studied the GAIM– and WAIM–molded curved tubes, and reported that the wall thickness was nonuniform at transitions. The thickness distribution as well as the hollow core ratio in WAIM–molded tubes strongly affected the mechanical property of molded parts. On the other hand, the axis asymmetry of wall thickness in the curved sections is found. Lin et al.[66] investigated the influence of mold temperature on the uniformity of residual wall thickness distribution at the curved sections of fluid-assisted injection-molded (FAIM) tubes. It was found that the uniformity of residual wall thickness in the FAIM parts could be improved by adopting differential mold temperatures, and the WAIM parts exhibited a more uniform thickness distribution at curved sections than the GAIM parts. When fluid (water or gas) penetrates the melt, it always seeks the path with the least resistance.[67] Nevertheless, for the WAIM process, the water occupies and reduces the shrinkage of the melt during packing stage. In the curved sections, the pressure difference between the water tips and melt fronts at all radii is the same, but it varies for the gas. Accordingly, the WAIM parts have a uniform thickness distribution.

Figure 6. Cross-section of WAIM parts with different cavities.[30] Copyright 2016, Wiley-VCH.

WAIM–molded plastic tubes with dimensional transitions were studied by Liu and Lin.[68] The results suggested that the water injection delay time and short shot size were the principal parameters affecting the hollowed core behavior of molded *d*–2*d*–*d* (a diameter *d* at the ends and a diameter 2*d* at the center portion) tubes, while the core-out geometries of the *d*–4*d*–*d* tubes were mainly influenced by the melt and mold temperatures, water pressure, water injection delay time, and melt short shot size. Additionally, the effects of different processing parameters on the surface gloss difference of WAIM parts were also performed.[57] They showed that the surface gloss difference mainly occurred at the rib/plate transition area of the WAIM parts and resulted from the roughness gradient of the part surface. Liu and Chen[69] demonstrated the shrinkage rate and the viscosity of the polymeric materials, and found that the void shapes of hollow cores mainly determined the water penetration lengths in the molded products. In addition, it was found that the WAIM parts exhibited less uniform void sizes along the water channel. Ahmadzai and Behravesh[61,70] claimed that the longest water penetration, the least wall thickness difference, the highest uniformity, and the lowest shrinkage were obtained at a longer holding time and higher mold temperature as well as an optimum delay time. In short, the water penetration behavior strongly influences the residual wall thickness of WAIM parts, which is mainly associated with the mold cavity, mold temperature, water pressure, and delay time.

The filling phenomena in FAIM were studied by Liu and Wu using a dynamic visualization technique.[71] The results showed that the WAIM–molded PP plates exhibited a more uniform hollow core ratio inside the plates than those molded by GAIM, and the water penetration was more stable than that of the gas penetration. During the postfilling of WAIM, the solidifying polymer underwent volumetric shrinkage, allowing water to penetrate into the parts. Liu and Huang[72] used a visualized

system to investigate the melt flow patterns and water penetration behavior during the melt filling. A mark between primary water penetration and secondary water penetration zones was observed. The studies demonstrated that the fountain flow phenomenon was seen under a lower initial filling. Moreover, it was found that the initial filling and water delay time, respectively, were the most significant factor affecting the water penetration length and the residual wall thickness. That is, an increase in initial filling and water delay time, respectively, led to a shorter water penetration length and a larger residual wall thickness. Additionally, Michaeli and Gründler[15] used glass vision mold and high-speed camera to observe double-channel structures and water inclusions in the WAIM parts. The formation of defects is affected by the heat transfer, and they can be avoided by setting the appropriate process parameters and adding surfactants to the water.

One major defect in WAIM part is the water fingering phenomenon (**Figure 7**) which can cause significant reduction in mechanical properties of the part. Liu et al.[73,74] investigated the effects of various processing parameters and water channel geometry including aspect ratio and fillet geometry on the fingering in the WAIM thermoplastic parts. It was found that the WAIM amorphous materials gave less fingering, while molded semicrystalline parts gave more fingering. The water pressure, water injection delay time, and short-shot size were found to be the principal parameters affecting the formation of water fingering, nevertheless, the temperature and the viscosity of the polymer melt were found to be very critical factors controlling the observed fingering effects.[61] In addition, Liu and Lin[75] found that WAIM–molded fiber-filled polymer parts have more severe water fingerings than the pure parts, and the water fingerings increased with increasing the filler content.

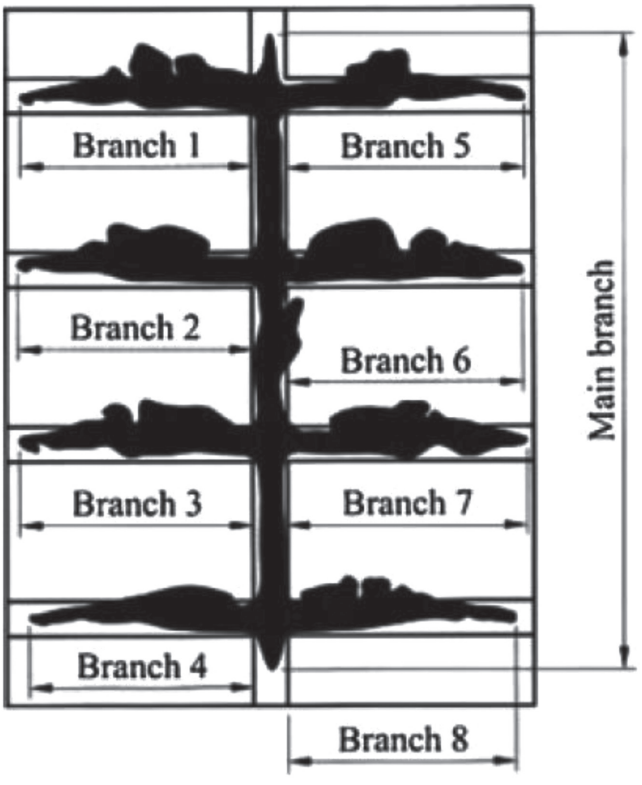

Figure 7. Schematic diagram of the water fingering in WAIM part.[73] Copyright 2006, Wiley-VCH.

Additionally, Michaeli proved the effect of gravity on the WAIM process, and suggested that one should fill in the cavity from bottom to top.[28] The temperature distributions in WAIM were measured using novel experimental set-ups which allowed the measurement of three-dimensional temperature fields in the depth of injection molding cavities throughout the molding cycles.[56,67] The results suggested that the shear heating by the viscous dissipation in the runners led to a significant increase of the melt temperature and should not be neglected in the process modeling and simulation.

3.3. Morphology and Orientation

It is well known that, in the injection molding process, polymer melt is subjected to an intricate thermo-mechanical field characterized by fast cooling rate and severe stress field, and such a thermomechanical history in return does play an important role in the development of morphological features.[76–80] The formation of orientation is a result of the competition between the flow induced orientation and its subsequent relaxation.[81–84] The morphology and orientation in the GAIM and CIM parts had been proved completely different.[85–89] In the WAIM process, polymer melt is confined not only by the mold wall but also by the injected water. Furthermore, during the WAIM process, melt is compelled to successively flow twice (i.e., the flow respectively brought by the melt filling and the injected water). More importantly, the injected water has a significant effect of rapid cooling rate on the interior melt. Obviously, it is unambiguous that the thermo-mechanical field in WAIM process is more complicated than that in GAIM and CIM processes.[23]

The hierarchical structure of high-density polyethylene (HDPE) molded by WAIM was studied by Liu et al.[23] using 2D small-angle X-ray scattering (2D-SAXS). The results showed that the WAIM part was characterized with a distinct skin–core–water channel structure through the thickness, including a shish-kebab structured skin, a typically spherulitic core, and a shish structure with low oriented lamellar water channel region (see **Figure 8**). A distinct skin–core–water channel structure was also observed.[24,25] Zheng and co-workers[26,27] studied the orientation and morphology of pure isotactic polypropylene (iPP) and nucleated iPP molded by WAIM. It was found that the introduction of nucleating agent (NA) notably influenced the hierarchical structure of WAIM parts. Additionally, the results showed that the orientation parameters obtained by 2D-SAXS decreased continuously from the skin surface to the core region, and then increased till at the water channel surface.[23,90] Those results demonstrate that water penetration and rapid cooling rate have a significant effect on the morphological features of the WAIM parts.

Huang and Deng[63] reported that the crystallinity of WAIM parts in the middle was higher than those from both outer and inner layers at a position near the water inlet. The samples taken from the outer layer, middle layer, and inner layer showed a similar melting peak and crystallinity at position near the end of water channel. Liu et al.[91,92] found that material at the mold-side

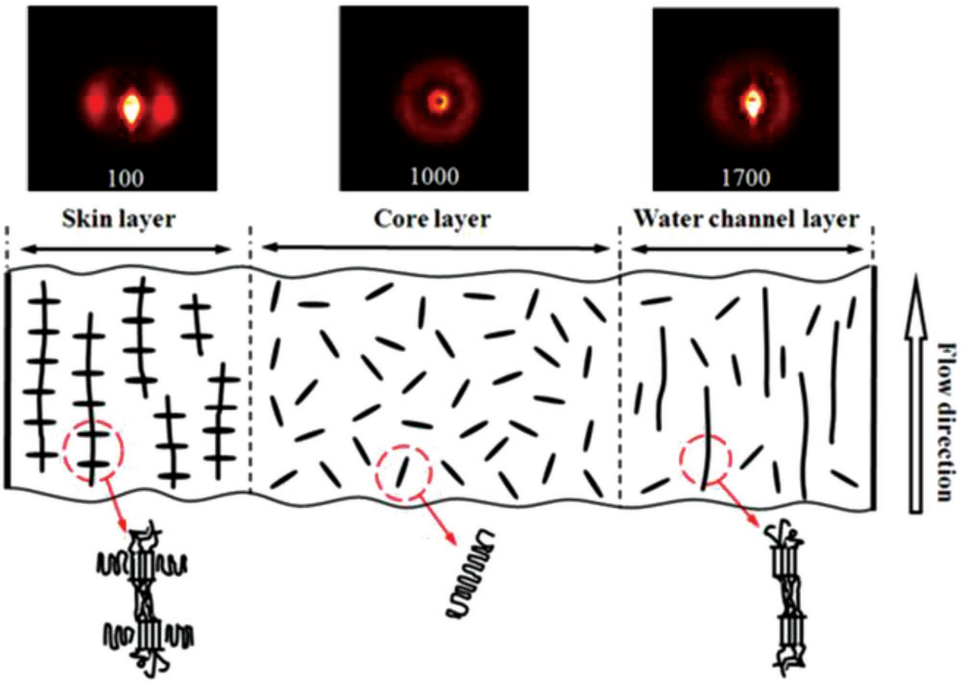

Figure 8. Selected 2D-SAXS image patterns in different regions and schematic of crystalline morphology for the WAIM part across the residual thickness.[23] Copyright 2012, Wiley-VCH.

exhibited a higher degree of crystallinity than that at the water-side, and the crystallinity at the water-side layer increased with increasing the water temperature, which was consistent with the reported results.[24] In addition, for the WAIM–molded nylon 6 (PA6) parts, it was found that the γ-phase crystals and α-phase crystals, respectively, dominated the crystal morphology at the skin and intermediate layers, but the coexistence of the γ- and the α-phase crystals dominated at the water-channel layer.[92]

It is well known that iPP is a polymorphic material with several crystal modifications, including monoclinic α-phase, trigonal β-phase, orthorhombic γ-phase, and smectic mesophase.[93–98] Thus, iPP is always used as a representative template to study the crystalline evolution during the injection molding process. Wang and Huang[99] suggested that lowering the melt temperature is favorable for the formation of β-form in the WAIM PP part (**Figure 9**a,b). However, Lin and Liu[24] reported that no β-form was found in the WAIM part, but a larger amount in the CIM part. They explained that this phenomenon was attributed to fast solidifying rate brought by the injected water that left short time for the growth of the β-phase on the formed α-row nuclei. In addition, for the WAIM PP/acrylonitrile–styrene copolymer (SAN) blend parts, it was found that high contents of β-form crystals (Figure 9c) and transcrystals (Figure 9d) were formed in the parts molded at relatively low melt temperatures. The formation of high contents of β-form crystals and the transcrystals is, respectively, due to the strong β-nucleating ability and in situ fibrillation of the SAN.

The molecular weight and the molecular weight distribution of polymers have a pronounced effect on the shear-induced crystallization.[100–103] It is generally believed that high molecular weight species play an important role in nucleation, melt orientation and subsequent crystallization. The crystal structures of the WAIM parts of PA6 with different molecular weights were investigated.[104] It was found that the molecular weight of the PA6 exhibited more effects on the formation of the γ-form as the cooling rate decreased. Moreover, the shear was found to hinder the formation of the γ-form for the PA6 with a higher molecular weight. Wang et al.[105] studied the crystal morphology of WAIM parts of HDPE with two different molecular weights. The results showed that the oriented lamellar structures were formed in the skin region and the spherulites were formed in the core and water channel regions for HDPE with higher molecular weight. But, for HDPE with a lower molecular weight, the spherulites were formed in all three regions at a position near the water inlet, whereas the oriented lamellar structures were formed in the skin region and the banded spherulites were dominant in other regions at a position near the end of the water channel. Although banded spherulites appear in low molecular weight HDPE, the studies are still consistent with the common view.

Recently, the results of Liu et al.[106] indicated that shish-kebab with high lamellar and molecular orientations was formed in the sample with a lower molecular weight rather than in a higher one, especially in the water channel layer (**Figure 10**). This finding is obviously inconsistent with the general consensus, that is, higher molecular weight polymer is much easier to form preferential orientation in the flow field than lower molecular weight one.[107,108] Such anomalous phenomenon is explained by the fact that even though the melts experienced the same processing, a lower shear rate was practically achieved in the higher molecular weight sample due to its high viscosity, which was in good agreement with the numerical simulation results by Hu et al.[109] The aforementioned results indicate that the flow history in the industrial processing method is far from what observed in the laboratory one.

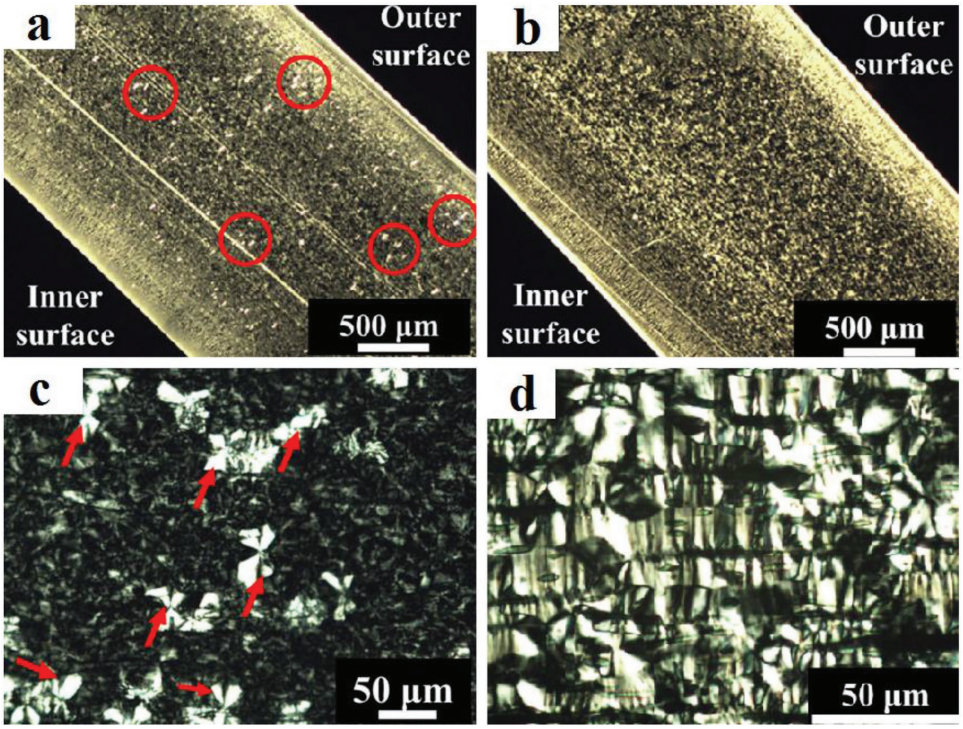

Figure 9. POM images of WAIM PP parts molded at a) low and b) high melt temperatures as well as c) core and d) inner layers of WAIM PP/SAN blend part.[99] Copyright 2013, Wiley-VCH.

3.4. Fiber-Filled Composites

The properties of the polymer composites depend on the filler (type, size, shape, orientation, and dispersion), matrix, interface between the filler and the polymer chains (the interface is important to provide a better load transfer), and so on.[110–120] Therefore, tremendous efforts have been devoted to developing the polymer composites with excellent desired properties.

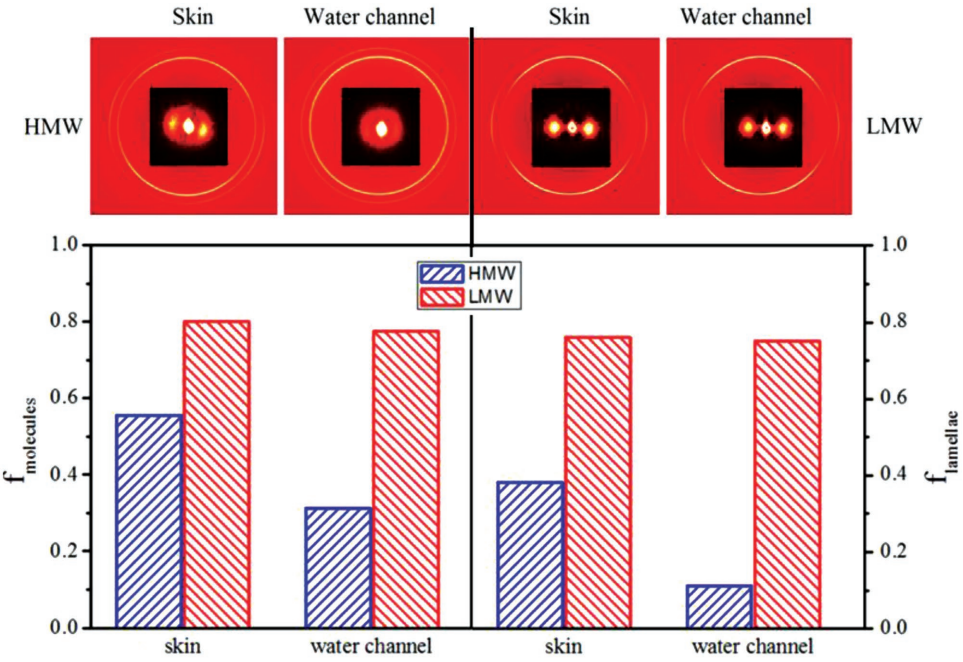

Figure 10. Two-dimensional wide-angle X-ray diffraction (2D-WAXD) and 2D-SAXS patterns of WAIM samples at different layers as well as the corresponding molecular and lamellar orientations.[106] Copyright 2013, Wiley-VCH.

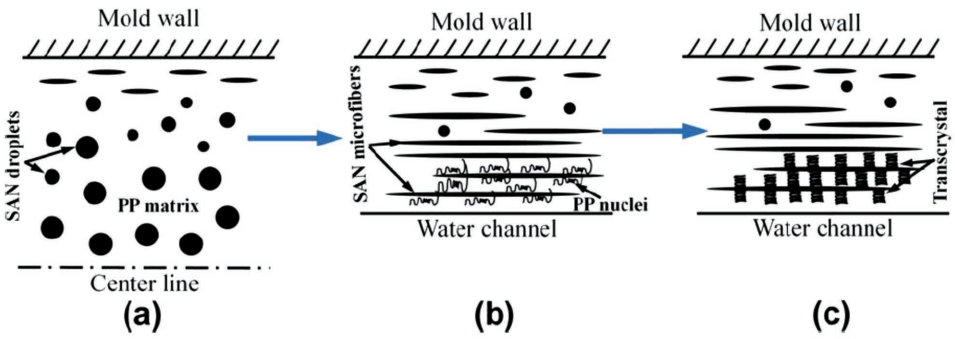

Figure 11. Schematic of formation mechanism of transcrystals during WAIM: a) short-shot stage; b) high-pressure water penetration stage; and c) water-assisted packing stage.[99] Copyright 2013, Wiley-VCH.

GF-filled composites have been widely used as structural materials in aerospace, marine, automobile, railways, civil engineering structures, and sporting goods due to their high specific strength and stiffness.[121–124] GF-filled composites molded by WAIM have the capability to produce parts having thick and thin sections with a good structural rigidity as well as to help to minimize the surface sink mark and warpage.[75] The successful commercialization of WAIM–molded GF-filled automotive duct was reported by Knights.[3] Liu and Chen[125] studied the moldability of GF-filled PP composites and optimized the length of water penetration by adopting a Taguchi method. It was found that fibers in WAIM parts were mostly oriented in the flow direction, especially in those areas near the mold/polymer and the polymer/water interfaces. This is due to the more severe shear involved during the mold filling, therefore the fibers are principally parallel to the flow direction. This finding is in good agreement with the GF-filled poly-butylene-terephthalate composites[91] and fiber-reinforced PP part.[126]

The surface roughness inside the water channel is the main problem for WAIM–molded GF-filled polymer composites. The agglomeration of fibers at some section of the formed water channel can block the path of water penetration. GF–reinforced PA6 composites exhibited rougher internal surfaces compared to those of virgin materials.[92] However, the inner surface roughness can be improved by increasing the water pressure. Lang and Parkinson[37] proposed a two-component WAIM method to improve the inner surface roughness.

Rib is usually designed to increase the stiffness of the WAIM parts and it also serves as water channels to guide the water penetration during the filling process. Nevertheless, water bubbles may penetrate outside of the designed rib and form finger-shape branches due to inappropriate mold design as well as processing parameters. Severe fingerings can result in a significant reduction in part stiffness. For example, Liu and Lin[75] investigated the fingering phenomenon in the WAIM–molded GF-filled PP composites under various processing parameters and water channel geometry. It was found that the water pressure, water injection delay time and melt short shot size were the principal parameters affecting the formation of water fingerings.

Recently, in situ microfibrillar-reinforced composites molded by WAIM were reported.[127–129] It was found that high shear stress and cooling rate caused by the high-pressure water penetration during the WAIM could result in the in situ fibrillation of the SAN droplet, followed by the formation of transcrystals at the interface between the SAN microfiber and PP matrix.[99] **Figure 11** shows the schematic of formation mechanism of transcrystals during the WAIM stages. Additionally, Michaeli et al.[12–14] found that the cooling time needed for WAIM–molded PP composites was shorter than that for GAIM composites. The yield strength of molded parts increased with increasing the mold temperature, but decreased with increasing the melt temperature.[92]

3.5. Polymer Blends

It is well known that the morphology development in the immiscible polymer blends is mainly controlled by the rheological and interfacial properties of the individual components, blend composition, processing conditions, and flow fields during processing.[130–134]

The phase morphological development in FAIM–molded HDPE/polycarbonate (PC) blends was studied by Lin and Liu.[24] It was observed that the shape and size of the dispersed phase depended on the position both across the part thickness and along the flow direction. Water-molded parts have a smaller PC particle distribution than gas (**Figure 12**). Additionally, high fluid pressures were found to mold parts with a smaller PC particle distribution. For example, Liu et al.[24,25] reported that the shape and size of the dispersed phase in the WAIM–molded HDPE/PA6 blends depended on the position both across the part thickness and along the flow direction, and high-water pressures were responsible for the small polyamide particle distribution. The small and large particles coexisted in the skin and water channel regions, indicating that both coalescence and disintegration of the dispersed phase occurred in these regions. Huang and Zhou[135] studied the WAIM–molded PP/PA6 blends, and found that the phase morphology varied across the residual wall of the WAIM curved ducts. Moreover, the morphologies developed at the position near the water inlet and near the end of the water channel were mainly ascribed to the melt filling and water penetration, respectively. It was demonstrated that higher water pressure, adequate melt temperature and higher injection speed resulted in a more obvious deformation of the dispersed PA6 phase.

Wang and Huang[136] reported the formation mechanism of crystal morphologies in the WAIM linear low-density

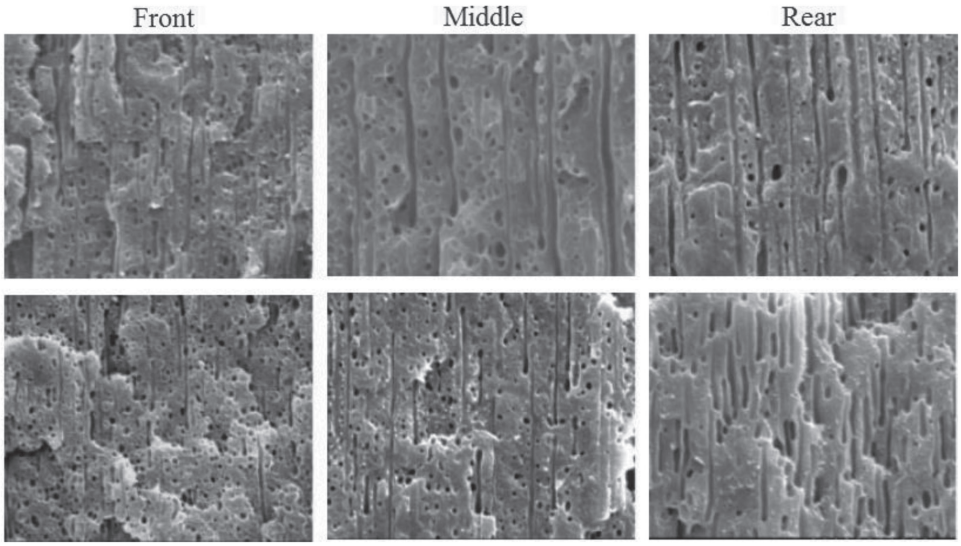

Figure 12. SEM images of skin layer of high pressure (up) GAIM and (down) WAIM–molded parts at different sections.[24] Copyright 2010, Wiley-VCH.

polyethylene (LLDPE)/HDPE blends, and found that the banded spherulites of LLDPE coexisted with the randomly oriented lamellae of HDPE for LLDPE/HDPE blends with a lower HDPE content at higher cooling rates, whereas a banding to nonbanding morphological transition occurred for LLDPE component at lower cooling rates. The banded spherulites were also found in the WAIM–molded low molecular weight HDPE parts.[84] The results indicated that the thermal effect and the heterogeneous nucleation effect of HDPE component were the main factors for the formation of crystal morphologies in the LLDPE/HDPE blends.

4. Conclusions and Perspectives

Processing technique is an important factor that determines the macroscopic properties of the prepared polymer materials in applications. However, the properties of a polymer product also depend on the polymer used and the capability to manipulate its internal morphology and structure. WAIM technology provides a new way to fabricate hollow and other complicated parts. Recent advances in study the WAIM were reviewed. It is widely accepted that the WAIM parts exhibit a skin–core–water channel structure, which is different from the skin–core structure in the CIM and GAIM parts. The studies indicate that the shear rate caused by water penetration, the higher cooling capacity, and incompressibility of the water, as well as additional nucleating agent contribute principally to the formation of oriented structure in the WAIM parts. In other words, the structural evolution in the WAIM parts is significantly influenced by the rapid cooling rate and shear brought by the injected water.

However, there are still many challenges about WAIM and some discussions are still not clear yet. For example, some other materials with high viscosity need be tested, including amorphous polymers and polymer composites. Some other approaches are needed suitable for improving the inner surface roughness of WAIM–molded polymer composites. How to predict and control the residual wall thickness of WAIM parts as well as how to avoid the formation of defects during the WAIM process are still challenges. On the other hand, the WAIM equipment cost should be further reduced, especially for the water injection unit. Additionally, the morphological and structural evolutions of WAIM–molded polyolefin parts in the presence of NAs as well as fillers are still unclear. Especially, the mutifunctions are desired to satisfy various applications including sensing, structural materials, energy, electromagnetic interference (EMI) shielding, environmental remediation, etc.[137–172] Therefore, additional efforts have to be made to further investigate and improve the WAIM technology for producing various nanocomposite parts.

Acknowledgements

The authors express their great thanks to the National Natural Science Foundation of China (11432003, 11572290) and the Startup Research Fund of Zhengzhou University (32210508) as well as the University Key Research Project of Henan Province (18A430031) for financial support.

Conflict of Interest

The authors declare no conflict of interest.

Keywords

residual wall thickness, water-assisted injection molding, water channels, water penetration

Received: January 15, 2018
Revised: March 29, 2018
Published online: June 4, 2018

[1] S. J. Liu, *Int. Polym. Process.* **2009**, *24*, 315.
[2] L. S. Turng, *J. Injection Molding Technol.* **2001**, *5*, 160.

[3] M. Knights, *Plast. Technol.* **2002**, *48*, 42.
[4] M. Knights, *Plast. Technol.* **2005**, *9*, 54.
[5] D. Oliveira, A. Mateus, P. Carreira, F. Simões, C. Malça, *Proc. Manuf.* **2017**, *12*, 141.
[6] E. Haberstroh, H. Wehr, *Macromol. Mater. Eng.* **2000**, *284*, 76.
[7] K. Himasekhar, L. S. Turng, V. W. Wang, H. H. Chiang, K. K. Wang, *Adv. Polym. Technol.* **1993**, *12*, 233.
[8] S. Y. Yang, S. J. Liou, W. N. Liou, *Adv. Polym. Technol.* **1997**, *16*, 175.
[9] L. S. Turng, *Adv. Polym. Technol.* **1995**, *14*, 1.
[10] W. Michaeli, A. Brunswick, T. Pohl, *Kunstst. Plast. Eur.* **1999**, *89*, 18.
[11] W. Michaeli, A. Brunswick, M. Gruber, *Kunstst. Plast. Eur.* **1999**, *89*, 84.
[12] W. Michaeli, A. Brunswick, C. Kujat, *Kunstst. Plast. Eur.* **2000**, *90*, 25.
[13] W. Michaeli, A. Brunswick, A. Pfannschmidt, *Kunstst. Plast. Eur.* **2002**, *92*, 38.
[14] W. Michaeli, T. Jüntgen, A. Brunswick, *Kunstst. Plast. Eur.* **2001**, *91*, 37.
[15] W. Michaeli, M. Gründler, *J. Polym. Eng.* **2011**, *31*, 417.
[16] W. Michaeli, O. Gronlund, C. Lettowsky, *Kunstst. Int.* **2006**, *96*, 121.
[17] W. Michaeli, C. Lettowsky, O. Gronlund, *Kunstst. Plast. Eur.* **2005**, *95*, 82.
[18] W. Michaeli, T. Jüntgen, O. Gronlund, A. Jain, *Kunstst. Plast. Eur.* **2004**, *94*, 67.
[19] A. Polynkin, L. Bai, J. F. T. Pittman, J. Sienz, L. Mulvaney-Johnson, E. Brown, A. Dawson, P. Coates, B. Brookshaw, K. Vinning, J. Butler, *Plast. Rubber Compos.* **2008**, *37*, 131.
[20] S. Sannen, M. De Munck, P. Van Puyvelde, J. De Keyzer, presented at *SPE EUROTEC*, Lyon, July **2013**.
[21] L. Silva, R. Lanrivain, W. Zerguine, A. Rodriguez-Villa, T. Coupez, *AIP Conf. Proc.* **2007**, *908*, 361.
[22] Z. Wang, H. Huang, B. Wang, *CIESC J.* **2013**, *64*, 1175.
[23] X. Liu, G. Zheng, Z. Jia, S. Li, C. Liu, Y. Zhang, C. Shao, K. Dai, B. Liu, Q. Zhang, S. Wang, C. Liu, J. Chen, Xi. Peng, C. Shen, *J. Appl. Polym. Sci.* **2012**, *125*, 2297.
[24] K. Y. Lin, S. J. Liu, *Macromol. Mater. Eng.* **2010**, *3*, 342.
[25] S. J. Liu, W. R. Lin, K. Y. Lin, *Polym. Adv. Technol.* **2011**, *22*, 2062.
[26] X. Liu, G. Zheng, K. Dai, Z. Jia, S. Li, C. Liu, J. Chen, C. Shen, Q. Li, *J. Mater. Sci.* **2011**, *46*, 7830.
[27] G. Zheng, Z. Jia, X. Liu, B. Liu, X. Zhang, K. Dai, C. Shao, X. Zheng, C. Liu, W. Cao, J. Chen, X. Peng, Q. Li, C. Shen, *Polym. Eng. Sci.* **2012**, *52*, 725.
[28] W. Michaeli, in *Injection Molding: Technology and Fundamental*, (Eds: M. Kamal, A. I. Isayev, S. J. Liu), Hanser Publishers, Munich, Germany **2009**, Ch. 6.
[29] S. J. Liu, Y. S. Chen, *Polym. Eng. Sci.* **2003**, *43*, 1806.
[30] T. Q. Kuang, K. Zhou, L. X. Wu, G. F. Zhou, L. S. Turng, *J. Appl. Polym. Sci.* **2016**, *133*, 42866.
[31] Y. Liu, T. Geng, L. Turng, C. Liu, W. Cao, C. Shen, Modelling Simul. *Mater. Sci. Eng.* **2017**, *25*, 065006.
[32] Y. Zhou, C. Shen, C. Liu, Q. Li, L. S. Turng, *J. Reinf. Plast. Compos.* **2010**, *29*, 76.
[33] M. Zhai, R. Zhang, Q. Li, C. Shen, *J. Plast. Film Sheet.* **2011**, *27*, 117.
[34] W. Cao, L. Kong, Q. Li, J. Ying, C. Shen, *Modell. Simul. Mater. Sci. Eng.* **2011**, *19*, 85003.
[35] Y. C. Wu, S. J. Liu, *Plast. Rubber Compos.* **2005**, *34*, 227.
[36] E. Bociaga, *Polimery* **2007**, *52*, 88.
[37] S. Lang, M. J. Parkinson, *Plast. Rubber Compos.* **2005**, *34*, 232.
[38] G. Q. Zheng, Q. Li, J. B. Chen, C. Y. Shen, W. Yang, M. B. Yang, *Polym.-Plast. Technol. Eng.* **2009**, *48*, 170.
[39] G. Q. Zheng, W. Yang, L. Huang, M. B. Yang, W. Li, C. T. Liu, C. Y. Shen, *Mater. Lett.* **2007**, *61*, 3436.
[40] F. Kamisli, M. E. Ryan, *Chem. Eng. J.* **1999**, *75*, 167.
[41] F. Kamisli, M. E. Ryan, *Chem. Eng. Sci.* **2001**, *56*, 4913.
[42] A. Polynkin, J. F. T. Pittman, J. Sienz, *Chem. Eng. Sci.* **2005**, *60*, 1591.
[43] T. Q. Kuang, B. P. Xu, G. F. Zhou, L. S. Turng, *J. Appl. Polym. Sci.* **2015**, *132*, 42468.
[44] Q. Li, W. Cao, S. Zhang, C. Shen, *IOP Conf. Ser. Mater. Sci. Eng.* **2010**, *10*, 012140.
[45] Z. Zhang, H. Zhou, Y. Gao, H. Yang, *Chin. J. Mech. Eng. (Engl. Ed.)* **2010**, *46*, 28.
[46] S. Zhang, W. Cao, G. Zheng, Z. Jia, C. Shen, *Int. Polym. Process.* **2011**, *26*, 560.
[47] J. G. Yang, X. H. Zhou, G. P. Luo. *Int. J. Adv. Manuf. Technol.* **2013**, *69*, 2605.
[48] J. G. Yang, X. H. Zhou, Q. Niu. *Int. J. Adv. Manuf. Technol.* **2013**, *67*, 367.
[49] J. G. Yang, X. H. Zhou, *J. Appl. Polym. Sci.* **2013**, *128*, 1987.
[50] J. G. Yang, X. H. Zhou, Q. Niu, *Int. Polym. Process.* **2012**, *5*, 584.
[51] T. Kuang, *Adv. Mater. Res.* **2011**, *179–180*, 1193.
[52] S. J. Liu, W. K. Chen, *Plast. Rubber Compos.* **2004**, *33*, 6.
[53] S. Sannen, P. Van Puyvelde, J. De Keyzer, *Adv. Polym. Technol.* **2015**, *34*, 21476.
[54] H. Zhou, Y. Chen, Z. Zhang, H. Yang, *Chin. J. Mech. Eng. (Engl. Ed.)* **2012**, *3*, 430.
[55] S. J. Liu, W. K. Chen, *Plast. Rubber Compos.* **2004**, *33*, 260.
[56] S. J. Liu, P. C. Su*Int. Polym. Process.* **2009**, *3*, 234.
[57] S. Sannen, M. DeMunck, P. Van Puyvelde, J. De Keyzer. *Int. Polym. Process.* **2012**, *5*, 602.
[58] S. Sannen, P. Van Puyvelde, J. De Keyzer, *Int. Polym. Process.* **2011**, *5*, 551.
[59] Y. C. Wu, K. M. Chen, S. J. Liu. *Plast. Rubber Compos.* **2006**, *35*, 425.
[60] S. J. Liu, Y. C. Wu, *Int. Polym. Process.* **2006**, *5*, 436.
[61] A. Z. Ahmadzai, A. H. Behravesh, *Polimery* **2009**, *54*, 564.
[62] K. Y. Lin, S. J. Liu, *Polym. Eng. Sci.* **2009**, *49*, 2257.
[63] H. X. Huang, Z. W. Deng, *J. Appl. Polym. Sci.* **2008**, *108*, 228.
[64] S. Y. Yang, P. T. Chu, *Adv. Polym. Technol.* **1999**, *18*, 11.
[65] S. J. Liu, M. H. Hsieh, *Int. Polym. Process.* **2007**, *1*, 82.
[66] K. Y. Lin, F. A. Chang, S. J. Liu, *Int. Commun. Heat Mass Transfer* **2009**, *36*, 491.
[67] S. J. Liu, P. C. Su, *Polym. Test.* **2009**, *28*, 66.
[68] S. J. Liu, C. H. Lin, *J. Reinf. Plast. Compos.* **2007**, *26*, 1441.
[69] S. J. Liu, Y. S. Chen, *Polym. Eng. Sci.* **2003**, *43*, 71
[70] A. Z. Ahmadzai, A. H. Behravesh, *Polimery* **2011**, *56*, 3.
[71] S. J. Liu, Y. C. Wu, *Polym. Test.* **2007**, *26*, 232.
[72] X. Liu, H. Huang, *AIChE Annu. Meet. Conf. Proc.* San Francisco, CA **2006**.
[73] S. J. Liu, S. P. Lin, *Adv. Polym. Technol.* **2006**, *25*, 98.
[74] S. J. Liu, Y. C. Wu, P. C. Lai. *Int. Polym. Process.* **2005**, *4*, 352.
[75] S. J. Liu, S. P. Lin, *Composites, Part A* **2005**, *36*, 1507.
[76] F. Luo, X. Liu, C. Shao, J. Zhang, C. Shen, Z. Guo. *Mater. Des.* **2018**, *144*, 25.
[77] Y. Wang, X. Liu, M. Lian, G. Zheng, K. Dai, Z. Guo, C. Liu, C. Shen, *Appl. Mater. Today* **2017**, *9*, 77.
[78] Z. Liu, X. Liu, G. Zheng, K. Dai, C. Liu, C. Shen, *J. Mater. Sci.* **2015**, *50*, 599.
[79] L. Huang, Z. Wang, G. Zheng, J. Guo, K. Dai, C. Liu, *Mater. Des.* **2015**, *78*, 12.
[80] Y. Pan, S. Shi, W. Xu, G. Zheng, K. Dai, C. Liu, J. Chen, C. Shen, *J. Mater. Sci.* **2014**, *49*, 1041.
[81] B. Chang, M. Xie, K. Dai, G. Zheng, S. Wang, C. Liu, J. Chen, C. Shen, *Polym. Test.* **2013**, *32*, 545.
[82] Y. Wang, M. Li, K. Wang, C. Shao, Q. Li, C. Shen, *Soft Matter* **2014**, *10*, 1512.
[83] Y. Wang, H. Zhang, M. Li, W. Cao, C. Liu, C. Shen, *Polym. Test.* **2015**, *41*, 163.
[84] X. Liu, Y. Pan, C. Peng, X. Hao, G. Zheng, D. W. Schubert, C. Liu, C. Shen, *Mater. Lett.* **2016**, *172*, 19.

[85] D. D. Xie, X. C. Xia, Y. H. Huang, R. Chen, B. H. Xie, M. B. Yang, *J. Appl. Polym. Sci.* **2017**, *134*, 45274.
[86] Y. Huang, X. Xia, Z. Liu, W. Yang, M. Yang, *Mater. Today Commun.* **2017**, *12*, 43.
[87] J. Hou, G. Zhao, G. Wang, G. Dong, J. Xu, *Mater. Des.* **2017**, *127*, 115.
[88] G. Zheng, W. Yang, B. Yin, M. Yang, C. Liu, C. Shen, *J. Appl. Polym. Sci.* **2006**, *102*, 3069.
[89] G. Zheng, W. Yang, L. Huang, Z. Li, M. Yang, B. Yin, Q. Li, C. Liu, C. Shen, *J. Mater. Sci.* **2007**, *42*, 7275.
[90] X. Liu, Y. Pan, G. Zheng, C. Liu, *RSC Adv.* **2016**, *6*, 68969.
[91] S. J. Liu, M. J. Lin, Y. C. Wu, *Compos. Sci. Technol.* **2007**, *67*, 1415.
[92] S. J. Liu, C. C. Shih, *J. Reinf. Plast. Compos.* **2008**, *27*, 985.
[93] B. Chang, B. Wang, G. Zheng, K. Dai, C. Liu, C. Shen, *Polym. Eng. Sci.* **2015**, *55*, 2714.
[94] X. Liu, M. Lian, Y. Pan, X. Wang, G. Zheng, C. Liu, D. W. Schubert, C. Shen, *Macromol. Mater. Eng.* **2018**, *303*, 1700465.
[95] Y. Pan, X. Liu, S. Shi, C. Liu, K. Dai, R. Yin, D. W. Schubert, G. Zheng, C. Shen, *Macromol. Mater. Eng.* **2016**, *301*, 1468.
[96] X. Liu, K. Dai, X. Hao, G. Zheng, C. Liu, D. W. Schubert, C. Shen, *Ind. Eng. Chem. Res.* **2013**, *52*, 11996.
[97] D. Mi, C. Xia, M. Jin, F. Wang, K. Shen, J. Zhang, *Macromolecules* **2016**, *49*, 4571.
[98] Z. Liu, X. Liu, G. Zheng, K. Dai, C. Liu, C. Shen, R. Yin, Z. Guo, *Polym. Test.* **2017**, *58*, 227.
[99] B. Wang, H. Huang, *Polym. Eng. Sci.* **2013**, *53*, 1927.
[100] S. Liang, H. Yang, K. Wang, Q. Zhang, R. N. Du, Q. Fu, *Acta Mater.* **2008**, *56*, 50.
[101] N. Sun, B. Yang, L. Wang, J. M. Feng, B. Yin, K. Zhang, M. B. Yang, *Polym. Int.* **2012**. *61*, 622.
[102] Q. P. Zhang, X. C. Xia, S. He, J. M. Feng, M. B. Yang, Y. T. Li, Y. L. Zhou, *Macromol. Mater. Eng.* **2015**, *300*, 901.
[103] Y. Ogino, H. Fukushima, G. Matsuba, N. Takahashi, K. Nishida, T. Kanaya, *Polymer* **2006**, *47*, 5669
[104] H. X. Huang, B. Wang, W. W. Zhou, *Composites, Part B* **2012**, *43*, 972.
[105] B. Wang, H. Huang, H. Lu, *J. Macromol. Sci. Part B: Phys.* **2011**, *50*, 1615.
[106] X. Liu, C. Zhang, K. Dai, G. Zheng, C. Liu, C. Shen, *Polym. Adv. Technol.* **2013**, *24*, 270.
[107] Y. An, L. Gu, Y. Wang, Y. M. Li, W. Yang, B. H. Xie, M. B. Yang, *Mater. Des.* **2012**, *35*, 633.
[108] W. Cao, K. Wang, Q. Zhang, R. N. Du, Q. Fu, *Polymer* **2006**, *47*, 6857.
[109] S. Hu, W. Yang, S. P. Liang, B. Yang, M. Yang, *J. Macromol. Sci. Part B: Phys.* **2009**, *48*, 1201.
[110] Y. Pan, X. Liu, J. Kaschta, X. Hao, C. Liu, D. W. Schubert, *Polymer* **2017**, *113*, 34.
[111] X. Wang, X. Liu, H. Yuan, H. Liu, C. Liu, T. Li, C. Yan, X Yan, C. Shen, Z. Guo, *Mater. Des.* **2018**, *139*, 372.
[112] C. Ji, M. Xie, B. Chang, K. Dai, B. Wang, G. Zheng, C. Liu, C. Shen, *Composites, Part A* **2013**, *46*, 26.
[113] X. Hao, J. Kaschta, Y. Pan, X. Liu, D. W. Schubert, *Polymer* **2016**, *82*, 57.
[114] X. Liu, Y. Pan, G. Zheng, D. W. Schubert, *Compos. Sci. Technol.* **2016**, *128*, 1.
[115] X. Liu, J. Krückel, D. W. Schubert, *Compos. Struct.* **2015**, *129*, 55.
[116] X. Liu, D. W. Schubert, *Compos. Struct.* **2016**, *136*, 414.
[117] Y. Wang, B. Tong, S. Hou, M. Li, C. Shen, *Composites, Part A* **2011**, *42*, 66.
[118] X. Liu, J. Krückel, G. Zheng, D. W. Schubert, *Compos. Sci. Technol.* **2014**, *100*, 99.
[119] M. Qu, F. Nilsson, Y. Qin, G. Yang, Y Pan, X. Liu, G. H. Rodriguez, J. Chen, C. Zhang, D. W. Schubert, *Compos. Sci. Technol.* **2017**, *150*, 24.
[120] X. Liu, J. Krückel, G. Zheng, D. W. Schubert, *ACS Appl. Mater. Interfaces* **2013**, *5*, 8857.
[121] M. Xie, B. Chang, H. Liu, K. Dai, G. Zheng, C. Liu, C. Shen, J. Chen, *Polym. Compos.* **2013**, *34*, 1250.
[122] B. Sun, Y. Qin, Y. Xu, Y. Sun, B. Wang, K. Dai, G. Zheng, C. Liu, J. Chen, *J. Mater. Sci.* **2013**, *48*, 5354.
[123] Q. Li, G. Zheng, K. Dai, M. Xie, C. Liu, B. Liu, X. Zhang, B. Wang, J. Chen, C. Shen, Q. Li, X. Peng, *Mater. Lett.* **2011**, *65*, 2274.
[124] J. K. Pandey, S. H. Ahn, C. S. Lee, A. K. Mohanty, *Macromol. Mater. Eng.* **2010**, *295*, 975.
[125] S. J. Liu, Y. S. Chen, *Composites, Part A* **2004**, *35*, 171.
[126] H. X. Huang, R. H. Zhou, C. Yang. *J. Compos. Mater.* **2012**, *47*, 183.
[127] B. Wang, H. X. Huang, Z. Y. Wang, *Composites, Part B* **2013**, *51*, 215.
[128] B. Wang, H. X. Huang, Z. Y. Wang, *Polym. Eng. Sci.* **2015**, *55*, 1698.
[129] B. Wang, H. X. Huang, Z. Y. Wang, *Acta Polym. Sin.* **2012**, *12*, 825.
[130] Y. Pan, X. Liu, J. Kaschta, C. Liu, D. W. Schubert, *J. Rheol.* **2017**, *61*, 759.
[131] Y. Pan, X. Liu, X. Hao, Z. Starý, D. W. Schubert, *Eur. Polym. J.* **2016**, *78*, 106.
[132] Y. Pan, X. Liu, X. Hao, D. W. Schubert, *Phys. Chem. Chem. Phys.* **2016**, *18*, 32125.
[133] O. D. Kwon, A. Zumbrunnen, *J. Appl. Polym. Sci.* **2001**, *82*, 1569.
[134] H. X. Huang, Y. F. Huang, X. J. Li, *Polym. Test.* **2007**, *26*, 770.
[135] H. X. Huang, R. H. Zhou, *Polym. Test.* **2010**, *29*, 235.
[136] B. Wang, H. X. Huang, *Polym. Eng. Sci.* **2012**, *52*, 117.
[137] X. Wu, J. Song, J. Li, Q. Shao, N. Cao, N. Lu, Z. Guo, *Polymer* **2017**, *124*, 41.
[138] Sun, P. Xie , Z. Wang, T. Su, Q. Shao, J. Ryu, X. Zhang, J. Guo, A. Shankar, J. Li, R. Fan, D. Cao, Z. Guo, *Polymer* **2017**, *125*, 50.
[139] J. Huang, Y. Cao, Q. Shao, X. Peng, Z. Guo, *Ind. Eng. Chem. Res.* **2017**, *56*, 10689.
[140] Y. Ma, L. Lyu, Y. Guo, Y. Fu, Q. Shao, T. Wu, S. Guo, K. Sun, X. Guo, E. K. Wujcik, Z. Guo, *Polymer* **2017**, *128*, 12.
[141] Y. Pan, X. Guo, G. Zheng, C. Liu, Q. Chen, C. Shen, X. Liu, *Macromol. Mater. Eng.* **2018**, *303*, 1800083.
[142] J. Zhao, L. Wu, C. Zhan, Q. Shao, Z. Guo, L. Zhang, *Polymer* **2017**, *133*, 272.
[143] X. Liu, Y. Pan, X. Hao, K. Dai, D. W. Schubert, *J. Appl. Polym. Sci.* **2016**, *133*, 43810.
[144] C. Wang, B. Mo, Z. He, C. X. Zhao, L. Zhang, Q. Shao, X. Guo, E. Eujcik, Z. Guo, *Polymer* **2018**, *138*, 363.
[145] C. Wang, Y. Wu, Y. Li, Q. Shao, X. Yan, C. Han, Z. Wang, Z. Liu, Z. Guo, *Polym. Adv. Technol.* **2018**, *29*, 668.
[146] Z. Hu, Q. Shao, Y. Huang, L. Yu, D. Zhang, X. Xu, J. Lin, H. Liu, Z. Guo, *Nanotechnology* **2018**, *29*, 185602.
[147] K. Sun, R. Fan, X. Zhang, Z. Zhang, Z. Shi, N. Wang, P. Xie, Z. Wang, G. Fan, H. Liu, C. Liu, T. Li, C. Yan, Z. Guo, *J. Mater. Chem. C* **2018**, *6*, 2925.
[148] Y. Guo, G. Xu, X. Yang, K. Ruan, T. Ma, Q. Zhang, J. Gu, Y. Wu, H. Liu, Z. Guo, *J. Mater. Chem. C* **2018**, *6*, 3004.
[149] C. Wang, Z. He, X. Xie, X. Mai, Y. Li, T. Li, M. Zhao, C. Yan, H. Liu, E. Wujcik, Z. Guo, *Macromol. Mater. Eng.* **2018**, *303*, 1700462.
[150] J. Lin, X. Chen, C. Chen, J. Hu, C. Zhou, X. Cai, W. Wang, C. Zheng, R. Zhang, J. Cheng, H. Liu, Z. Guo, *ACS Appl. Mater. Interfaces* **2018**, *10*, 6124.
[151] Y. Li, B. Zhou, G. Zheng, X. Liu, T. Li, C. Yan, C. Cheng, K. Dai, C. Liu, C. Shen, Z. Guo, *J. Mater. Chem. C* **2018**, *6*, 2258.
[152] Y. Wei, Z. Li, X. Liu, K. Dai, G. Zheng, C. Liu, J. Chen, C. Shen, *Colloid Polym. Sci.* **2014**, *292*, 2891.
[153] Y. Zhang, M. Zhao, J. Zhang, Q. Shao, J. Li, H. Li, B. Lin, M. Yu, S. Chen, Z. Guo, *J. Polym. Res.* **2018**, *25*, 130.
[154] J. Jiang, X. Liu, M. Lian, Y. Pan, Q. Chen, H. Liu, G. Zheng, Z. Guo, D. Schubert, C. Shen, C. Liu, *Polym. Test.* **2018**, *67*, 183.

[155] H. Liu, W. Huang, X. Yang, K. Dai, G. Zheng, C. Liu, C. Shen, X. Yan, J. Guo, Z. Guo, *J. Mater. Chem. C* **2016**, *4*, 4459.
[156] H. Liu, M. Dong, W. Huang, J. Gao, K. Dai, J. Guo, G. Zheng, C. Liu, C. Shen, Z. Guo, *J. Mater. Chem. C* **2017**, *5*, 73.
[157] X. Guan, G. Zheng, K. Dai, C. Liu, X. Yan, C. Shen, Z. Guo, *ACS Appl. Mater. Interfaces* **2016**, *8*, 14150.
[158] H. Kang, Q. Shao, X. Guo, A. Galaska, Y. Liu, Z. Guo, *Eng. Sci.* **2018**, *1*, 78.
[159] C. Hu, Z. Li, Y. Wang, J. Gao, K. Dai, G. Zheng, C. Liu, C. Shen, H. Song, Z. Guo, *J. Mater. Chem. C* **2017**, *5*, 2318.
[160] Z. Hu, C. Wang, F. Zhao, X. Xu, S. Wang, L. Yu, D. Zhang, Y. Huang, *Nanoscale* **2017**, *9*, 8825.
[161] H. Gu, H. Zhang, J. Lin, Q. Shao, D. P. Young, L. Sun, T. D. Shen, Z. Guo, *Polymer* **2018**, *143*, 324.
[162] Y. Pan, D. W. Schubert, J. E. Ryu, E. Wujick, C. Liu, C. Shen, X. Liu, *Eng. Sci.* **2018**, *1*, 86.
[163] a) H. Gu, C. Liu, J. Zhu, J. Gu, E. Wujcik, L, Shao , N. Wang, H. Wei, R. Scaffaro, J. Zhang, Z. Guo, *Adv. Compos. Hybrid Mater.* **2018**, *1*, 1; b) X. Cui, G. Zhu, Y. Pan, Q. Shao, C. Zhao, M. Dong, Y. Zhang, Z. Guo, *Polymer* **2018**, *138*, 203.
[164] H. Liu, Y. Li, K. Dai, G. Zheng, C. Liu, C. Shen, X. Yan, J. Guo, Z. Guo, *J. Mater. Chem. C* **2016**, *4*, 157.
[165] L. Yan, H. Wang, D. Huang, H. Luo, *Eng. Sci.* **2018**, *1*, 4.
[166] Q. Chen, J. Jing, H. Qi, I. Ahmed, H. Yang, X. Liu, T. Lu, A. R. Boccaccini, *ACS Appl. Mater. Interfaces* **2018**, *10*, 11529.
[167] Z. Lu, Y. Pan, X. Liu, G. Zheng, D. W Schubert, C. Liu, *Mater. Lett.* **2018**, *221*, 62.
[168] X. Hao, J. Kaschta, X. Liu, Y. Pan, D. W. Schubert, *Polymer* **2015**, *80*, 38.
[169] C. Wang, M. Zhao, J. Li, J. Yu, S. Sun, S. Ge, X. Guo, F. Xie, B. Jiang, E. Wujcik, Y. Huang, N. Wang, Z. Guo, *Polymer* **2017**, *131*, 263.
[170] C. Feng, L. Bai, R. Bao, Z. Liu, M. Yang, J. Chen, W. Yang, *Adv. Compos. Hybrid Mater.* **2018**, *1*, 160.
[171] X. Cheng, Z. Wang, X. Jiang, T. Li, C. Lau, Z. Guo, J. Ma, L. Shao, *Prog. Mater. Sci.* **2018**, *92*, 258.
[172] Z. Hu, D. Zhang, L. Yu, Y. Huang, *J. Mater. Chem. B* **2018**, *6*, 518.